The analysis of cylindrical orthotropic curved bridge decks

Autor(en): **Cheung, Yau Kai**

Objekttyp: **Article**

Zeitschrift: **IABSE publications = Mémoires AIPC = IVBH Abhandlungen**

Band (Jahr): **29 (1969)**

PDF erstellt am: **21.09.2024**

Persistenter Link: https://doi.org/10.5169/seals-22918

The Analysis of Cylindrical Orthotropic Curved Bridge Decks

Calcul des tabliers de ponts courbes à orthotropie circulaire

Die Berechnung kreisförmig-orthotroper, gekrümmter Brückenplatten

YAU KAI CHEUNG
Ph. D., MICE., Associate Professor of Civil Engineering, University of Calgary, Calgary, Alberta, Canada

Introduction

The rapid development of the modern highway interchanges required the use of more and more curved structures. Such structures are usually either plain curved slabs or are made up of a system of slabs and multiple stiffening girders. These multiple girders are usually arranged orthogonally along the radii and arcs of concentric circles, and can be treated as an equivalent cylindrical orthotropic plate [1, 2]. Much of the research conducted in this field so far are on curved girder bridges, in which the structure is analysed either as a curved beam or an assemblage of curved beams, although COULL and DAS [3] made some experimental and theoretical investigations into the behaviour of uniform thickness isotropic curved slab bridges, while CERADINI [4] attemted the approximate solution of an orthotropic bridge for a line loading with a simple sinusoidal variation. The most advanced work done on this topic appears to be due to a paper by YONEZAWA [5], in which he studied the static and dynamic behaviour of curved orthotropic bridges with edge girders. Unfortunately, the analysis is only valid for uniformly distributed loads and constant thickness slabs.

The finite strip method developed by the author has been applied successfully to the analysis of orthotropic right bridges [6]. In this paper, the method is extended to solve also the problem of orthotropic curved bridges. In fact, it will be demonstrated that any right bridge deck can be analysed by the same computer programme by simply adopting a very small subtended angle together with a large radius.

In this method, the bridge is divided into a number of concentric circular strips, each strip being simply-supported at its two ends. A displacement function of the form $\phi(r)\,\psi(\theta)$ is chosen for the strip, in which $\phi(r)$ is a beam function with undetermined parameters, and $\psi(\theta)$ is a Fourier series which satisfy automatically the support conditions. A stiffness matrix can be developed and the whole bridge is then analysed by the standard stiffness approach. The advantage of this method over conventional finite element method lies in the fact that a two-dimensional problem is now reduced into a one-dimensional one, with the result that a very compact narrow band matrix with a small number of unknowns is used in the analysis. Because of this simplification the computer programme for such an approach is comparatively short and also little input data is required for its execution.

Problems involving interior or edge beams can be included in the same way as indicated in a previous paper [6].

Analysis

A. Displacement Function

The bridge is now assumed to be divided into a number of curved strips, each strip having constant orthotropic properties of its own, but can differ from adjacent strips so as to approximate radially variable property problems. Such a strip can be found in Fig. 1.

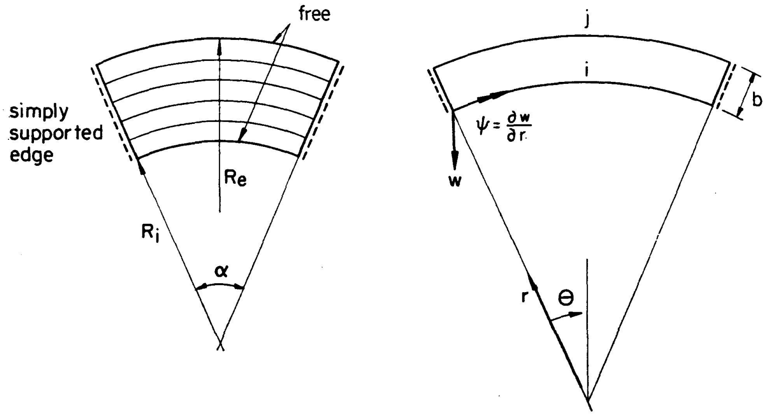

Fig. 1. Curved bridge and typical strip.

The boundary conditions for each strip are:

at $\theta=0$ and $\theta=\alpha$

$$w = 0 \quad \text{and} \quad M_\theta = -D_\theta \frac{1}{r}\left(\frac{1}{r}\frac{\partial^2 w}{\partial\theta^2} + \frac{\partial w}{\partial r}\right) - \nu_r D_\theta \frac{\partial^2 w}{\partial r^2} = 0, \tag{1a}$$

at $r=r_i$

$$w = w_i, \qquad \psi = \left(\frac{\partial w}{\partial r}\right)_i = \psi_i, \tag{1b}$$

at $r=r_j$

$$w = w_j, \qquad \psi = \left(\frac{\partial w}{\partial r}\right)_j = \psi_j. \tag{1c}$$

The polar coordinates (r, θ) are obviously suitable for this problem, while further simplification can be achieved by introducing a dimensionless parameter $R = \frac{r - r_i}{b}$, in which $b = \frac{r_j - r_i}{2}$. Thus we have at $r = r_i$, $R = 0$ and at $r = r_j$, $R = 2$.

A suitable deflection function in terms of the parameters R and θ, and satisfying all the boundary conditions can be given as

$$w = \sum_{m=1,2\dots\infty} \left[\left(1 - \frac{3}{4}R^2 + \frac{1}{4}R^3\right) w_{im} + b\left(R - R^2 + \frac{R^3}{4}\right) \psi_{im} + \left(\frac{3}{4}R^2 - \frac{1}{4}R^3\right) w_{jm} + b\left(\frac{R^3}{4} - \frac{R^2}{2}\right)\psi_{jm}\right] \sin\frac{m\pi\theta}{\alpha}, \tag{1d}$$

where w_{im}, ψ_{im} etc. are the generalized displacement parameters of the mth term along the sides of the strip. In general it is neither possible nor necessary to use an infinite number of terms, and depending on the nature of the loading, three to eight terms have always been found to give accurate results.

The deflection function given in Eq. (1d) is a compatible function, since all function values and its first partial derivatives along the common boundary of two adjacent strips will match uniquely.

Eq. (1d) can be written matrically as

$$w = C\,W = [C_1\,C_2 \dots C_k]\begin{Bmatrix} W_1 \\ W_2 \\ \vdots \\ W_k \end{Bmatrix} = \sum_1^k C_m\,W_m, \tag{2}$$

in which

$$C_m = \left[\left(1 - \frac{3}{4}R^2 + \frac{1}{4}R^3\right),\ b\left(R - R^2 + \frac{R^3}{4}\right),\ \left(\frac{3}{4}R^2 - \frac{1}{4}R^3\right),\ b\left(\frac{R^3}{4} - \frac{R^2}{2}\right)\right] \sin\frac{m\pi\theta}{\alpha}$$

and $W_m = \{w_{im}\,\psi_{im}\,w_{jm}\,\psi_{jm}\}^T$.

B. Stiffness and Load Matrices

The curvatures of a plate in polar coordinates are given by [7]

$$\chi = \begin{Bmatrix} -\chi_r \\ -\chi_\theta \\ 2\chi_{r\theta} \end{Bmatrix} = \begin{Bmatrix} -\dfrac{\partial^2 w}{\partial r^2} \\ -\dfrac{1}{r}\left(\dfrac{1}{r}\dfrac{\partial^2 w}{\partial \theta^2} + \dfrac{\partial w}{\partial r}\right) \\ -\dfrac{2}{r}\left(\dfrac{\partial^2 w}{\partial r\,\partial\theta} - \dfrac{1}{r}\dfrac{\partial w}{\partial \theta}\right) \end{Bmatrix} = \sum_1^k B_m\,W_m. \tag{3}$$

B_m can be obtained by differentiating C_m with respect to r and θ, and its explicit form is given in Appendix I.

The moment matrix for cylindrical orthotropic plates can be found in the same text [7], and we have

$$M = \begin{Bmatrix} M_r \\ M_\theta \\ M_{r\theta} \end{Bmatrix} = \begin{bmatrix} D_r & \nu_\theta D_r & 0 \\ \nu_r D_\theta & D_\theta & 0 \\ 0 & 0 & D_k \end{bmatrix} \begin{Bmatrix} -\chi_r \\ -\chi_\theta \\ 2\chi_{r\theta} \end{Bmatrix} = \sum_1^k D\, B_m\, W_m. \tag{4}$$

Here D_r, D_θ are bending rigidities for directions r and θ; D_k is the twisting rigidity:

$$D_r = \frac{E_r t^3}{12(1-\nu_r \nu_\theta)}, \qquad D_\theta = \frac{E_\theta t^3}{12(1-\nu_r \nu_\theta)}, \qquad D_k = \frac{G_{r\theta} t^3}{12}.$$

For an isotropic material

$$D_r = D_\theta = D = \frac{E t^3}{12(1-\nu^2)}, \qquad D_k = \frac{1-\nu}{2} D.$$

The expression for the total potential energy of each strip is given by

$$\begin{aligned} U &= \tfrac{1}{2}\int_0^\alpha \int_{r_i}^{r_j} (-M_r\chi_r - M_\theta\chi_\theta + 2M_{r\theta}\chi_{r\theta})\, r\, dr\, d\theta \\ &\quad - \int_0^\alpha \int_{r_i}^{r_j} W^T q\, r\, dr\, d\theta - \int_0^\alpha \{w_i \psi_i w_j \psi_j\}\{P_i M_i P_j M_j\}^T r\, d\theta, \end{aligned} \tag{5}$$

in which the first integral denotes the strain energy of the strip, the second integral the work done by distributed surface loads, and the third integral the work done by edge forces acting along the sides of the strips.

Substituting (3) and (4) into (5)

$$\begin{aligned} U &= \tfrac{1}{2}\int_0^\alpha \int_{r_i}^{r_j} M^T \chi\, r\, dr\, d\theta - \int_0^\alpha \int_{r_i}^{r_j} W^T C^T q\, r\, dr\, d\theta - \int_0^\alpha \{w_i \psi_i w_j \psi_j\}\{P_i M_i P_j M_j\}^T r\, d\theta = \\ &\tfrac{1}{2}\int_0^\alpha \int_{r_i}^{r_j} W^T B^T D\, B\, W\, r\, dr\, d\theta - \int_0^\alpha \int_{r_i}^{r_j} W^T C^T q\, r\, dr\, d\theta \\ &- \sum W_m^T \int_0^\alpha \sin\frac{m\pi\theta}{\alpha}\{P_i M_i P_j M_j\}^T r\, d\theta. \end{aligned} \tag{6}$$

If the load q is also resolved into a sine series in the circumferential direction similar to the deflexion function, then

$$q = q_1 \sin\frac{\pi\theta}{\alpha} + q_2 \sin\frac{2\pi\theta}{\alpha} + \cdots + q_k \sin\frac{k\pi\theta}{\alpha} = \sum_1^k q_n \sin\frac{n\pi\theta}{\alpha}, \tag{7}$$

where
$$q_n = \frac{\int_c^d q \sin\frac{n\pi\theta}{\alpha} r\, d\theta}{\int_0^\alpha \sin^2\frac{n\pi\theta}{\alpha} r\, d\theta}$$
for distributed loads from $\theta = c$ to $\theta = d$

and
$$q_n = \frac{P \sin\frac{n\pi c}{\alpha}}{\int_0^\alpha \sin^2\frac{n\pi\theta}{\alpha} r\, d\theta}$$
for a concentrated load P at $\theta = c$.

Eq. (6) can now be written as

$$U = \sum_{\substack{m=1,k\\n=1,k}}\sum \left[\tfrac{1}{2} W_m^T \left(\int_0^{\alpha}\int_{r_i}^{r_j} B_m^T D\, B_n\, r\, dr\, d\theta\right) W_m - W_m^T \int_0^{\alpha}\int_{r_i}^{r_j} \left(C_m^T q_n \sin\frac{n\pi\theta}{\alpha}\right) r\, dr\, d\theta \right.$$
$$\left. - W_m^T \int_0^{\alpha} \sin\frac{m\pi\theta}{\alpha} \sin\frac{n\pi\theta}{\alpha} \{P_{in}\, M_{in}\, P_{jn}\, M_{jn}\}^T r\, d\theta\right]. \tag{8}$$

The integrals with respect to θ are all orthogonal and therefore each term of the series can be treated individually and then summed to give the final results. Therefore only one typical term will be used in all subsequent derivation.

Differentiating Eq. (7) with respect to the generalized displacements of each term one after the other and equating each of the differentials to zero will yield a set of 4 simultaneous equations.

$$\frac{\partial U}{\partial W_m} = \left\{\frac{\partial U}{\partial w_{im}}\,\frac{\partial U}{\partial \psi_{im}}\,\frac{\partial U}{\partial w_{jm}}\,\frac{\partial U}{\partial \psi_{jm}}\right\}^T = \int_0^{\alpha}\int_{r_i}^{r_j} B_m^T D\, B_m\, r\, dr\, d\theta\, W_m$$
$$-\int_0^{\alpha}\int_{r_i}^{r_j} C_m^T q_m \sin\frac{m\pi\theta}{\alpha} r\, dr\, d\theta - \int_0^{\alpha} \{P_{im}\, M_{im}\, P_{jm}\, M_{jm}\}^T \sin^2\frac{m\pi\theta}{\alpha} r\, d\theta = \tag{9}$$
$$S_m W_m - F_{qm} - F_{pm} = 0.$$

S_m is a square symmetric matrix similar in form to a stiffness matrix and F_{qm}, F_{pm} to load matrices in structural analysis. In the present computer program these matrices are obtained by numerical integration.

The stiffness matrix of a generalized finite element is always singular and cannot be inverted, while here S_m is no longer singular due to the pre-set conditions. As a result of this, the coefficients along a row or column of the matrix for a particular force component will now no longer add up to zero.

Overall Stiffness Matrix and its Solution

The final equations for minimizing the total potential energy of the whole bridge can be obtained by summing up the contributions from the individual strips, similar to assembly procedure of beam stiffness matrices. The resulting equations are solved by a narrow band matrix solution technique to yield the nodal displacement parameters, which in turn will give the internal moments of each strip when used in conjunction with Eq. (4). The results of each term are then summed automatically by the computer to give the final results.

Numerical Examples and Discussions

The first example attempted deals with the analysis of uniform thickness isotropic curved bridges, and the theoretical and experimental results obtained by COULL and DAS [3] are used as a check on the accuracy of the present method. Two model bridge slabs of both perspex and asbestos-cement, each with an included angle of 60°, are loaded with central point loads at three different radial positions, the inner and outer edges, and at mid-radius respectively. A comparison of the deflections and bending moments along the central section are given in Figs. 2—4. In general, there is good agreement between all sets of results. The finite strip method consistently gives higher moments under the load points when sufficient number of terms are taken (8 terms in this case). However, if only 3 terms are used, the maximum values then are much closer to the theoretical results of Coull and Das, who also took only 3 terms for their analysis. A point of interest is that the higher terms (i. e., after the 3rd or 4th term) only affect results in the very vicinity of the point load.

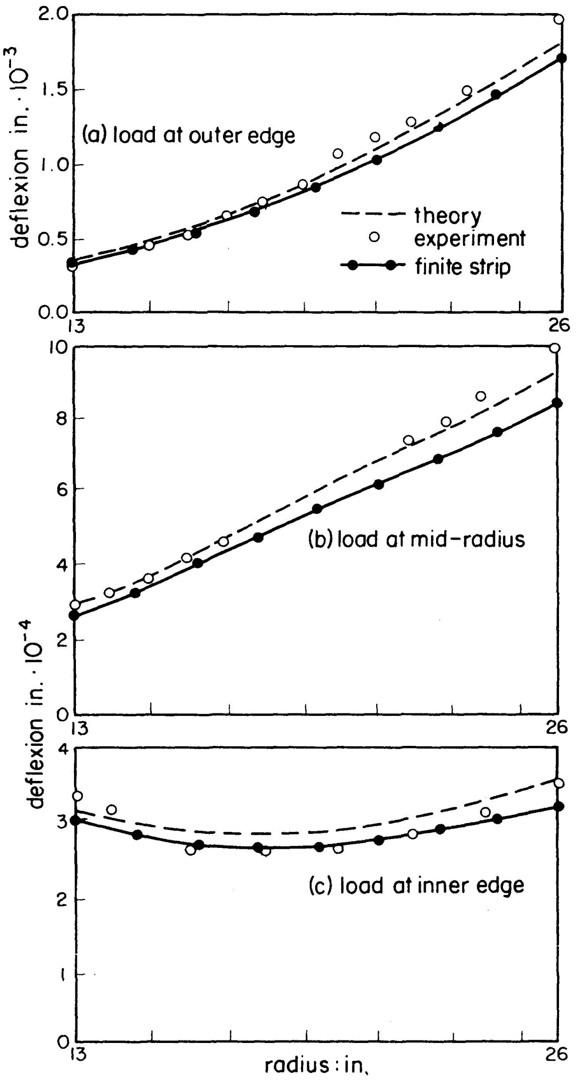

Fig. 2. Radial distributions of mid-span deflexions due to unit load at (a) outer edge, (b) mid-radius, (c) inner edge; asbestos-cement model.

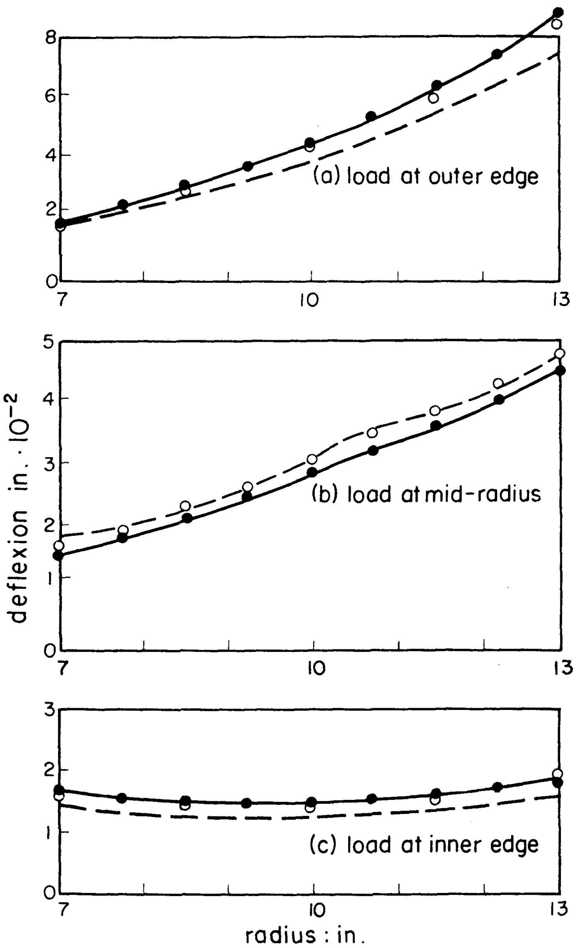

Fig. 3. Radial distributions of mid-span deflexions due to unit load at (a) outer edge, (b) mid-radius, (c) inner edge; perspex model.

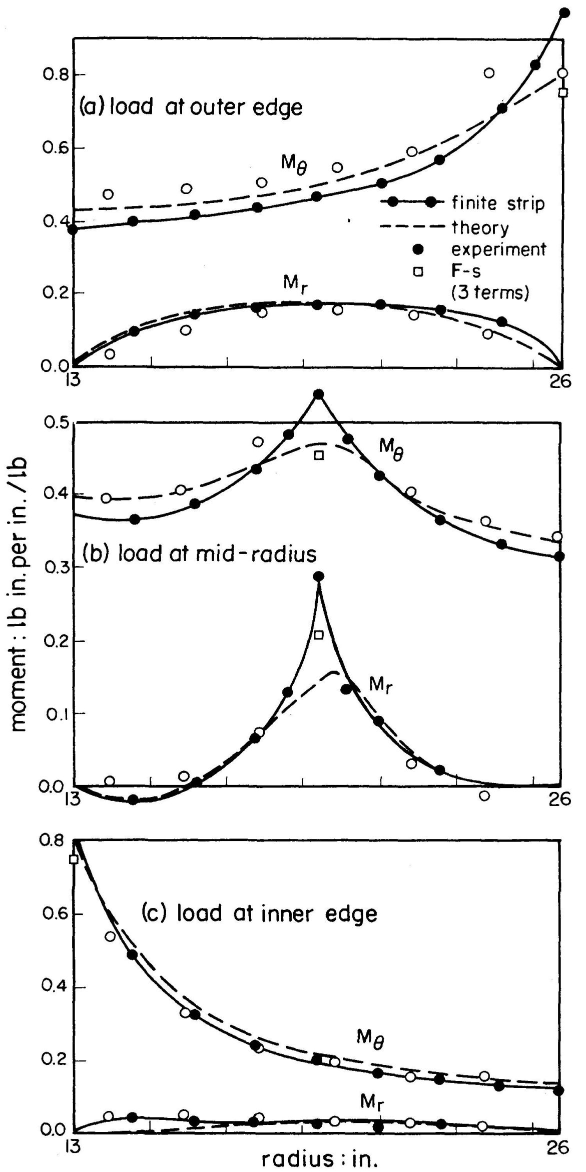

Fig. 4. Distributions of tangential and radial bending moments at mid-span due to load at (a) outer edge, (b) mid-radius, (c) inner edge; asbestos-cement model.

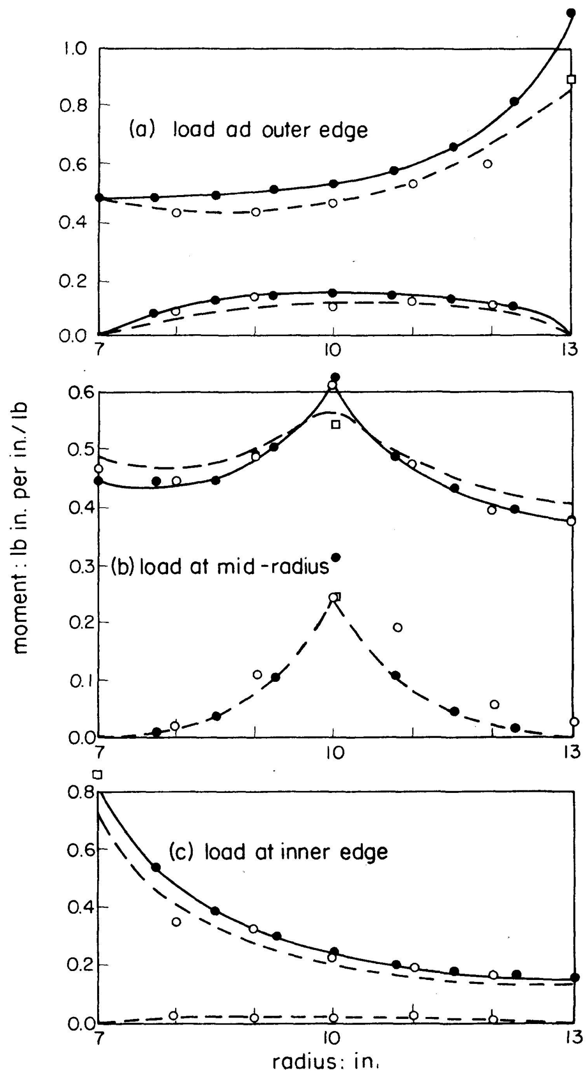

Fig. 5. Distributions of tangential and radial bending moments at mid-span due to load at (a) outer edge, (b) mid-radius, (c) inner edge; perspex model.

A typical run for one loading, using 8 terms and 8 strips, took under half a minute on the medium speed IBM 360-50 computer.

For bridges with cylindrical orthotropy, a similar comparison to that made in the previous example is not possible because of the lack of relevant experimental data. It is therefore decided to test the computer programme by analysing a cylindrical orthotropic bridge with a very small subtended angle but a very large radius, and then compare the results with those obtained from an orthotropic right bridge program, the accuracy of which has been proved beyond doubt. The geometric data for the various cases are as follows:

Table I. Comparison of deflections and moments (4 terms) along central section

	at R_i			at mid-radius			at R_e		
	w	M_r	M_θ	w	M_r	M_θ	w	M_r	M_θ
$D_x = 1$, $D_y = 9$, $D_1 = 0$, $D_{xy} = 1.5$ Square Bridge	0.001306	0.1163	0.001176	0.003475	0.4698	0.1097	0.001306	0.1163	0.001176
$D_r = 1$, $D_\theta = 9$, $\nu_r = 0$, $\nu_\theta = 0$, $D_k = 1.5$									
Case (I)	0.001297	0.1160	0.001180	0.003475	0.4698	0.1097	0.001315	0.1167	0.001172
Case (II)	0.001288	0.1157	0.001184	0.003475	0.4699	0.1097	0.001324	0.1171	0.001168
Case (III)	0.001270	0.1150	0.001193	0.003475	0.4699	0.1097	0.001343	0.1178	0.001160

I. $R_i = 199.5$, $R_e = 200.5$, $\alpha = 0.006$ radian,
II. $R_i = 99.5$, $R_e = 100.5$, $\alpha = 0.01$ radian,
III. $R_i = 49{,}5$, $R_e = 50.5$, $\alpha = 0.02$ radian.

The point in common is that the circumferential length at mid-radius and also the length $(R_e - R_i)$ are always equal to unity.

The results for the various bridges under a central point load are summarized in Table I. It should be noted that the results of the right bridge are nearly identical with those of case (I), while cases (II) and (III) also give nearly the same values, but with the unmistakable tendency to become more flexible at the external radius side with progressive curvature.

The last example demonstrates the versatility of the method. An imaginary bridge of the same dimension as the perspex model and with abrupt change in thickness is analysed under dead load. It should be mentioned that the input data required for this case is no more than that for a uniform thickness case, since each strip always contains its individual bending and torsional rigidities. Only three terms of the series are needed in this analysis, because convergence is very rapid for uniformly distributed loading. The deflexions and bending moments for the central section are plotted in Fig. 6.

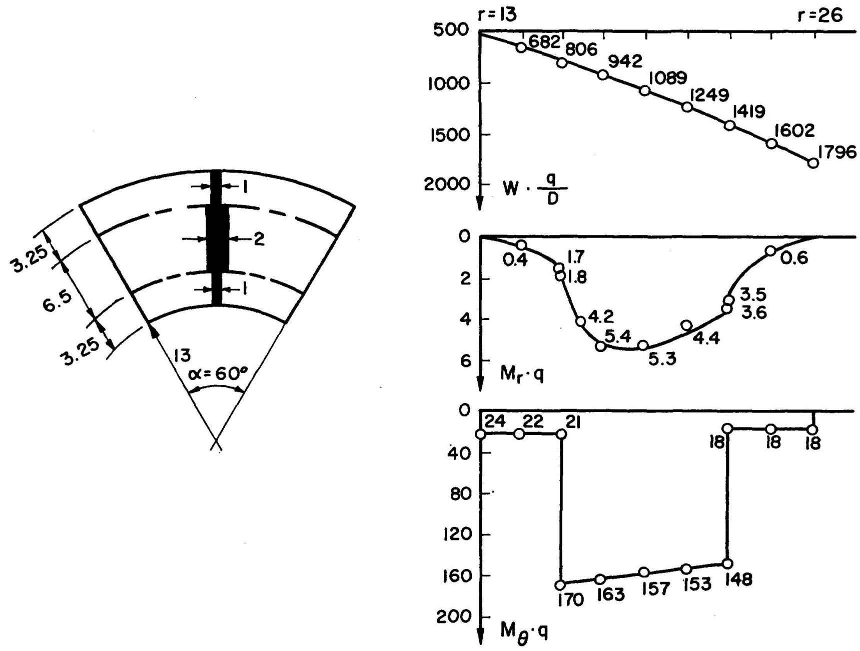

Fig. 6. Distribution of deflections and moments at midspan of variable thickness bridge under dead load.

Conclusion

It has been demonstrated that the finite strip method is an ideal tool for the analysis of curved bridges with cylindrical orthotropic properties. This method is simple in concept, easy to program, requires minimal input data, fairly small computer storage and little time to run.

Appendix I. Curvature-Displacement Matrix

$\left(-\frac{3R}{2b^2}+\frac{3}{2b^2}\right)S$	$\left(\frac{2}{b}-\frac{3R}{2b}\right)S$	$\left(\frac{3R}{2b^2}-\frac{3}{2b^2}\right)S$	$\left(\frac{1}{b}-\frac{3R}{2b}\right)S$
$\frac{1}{r^2}\left(1-\frac{3}{4}R^2+\frac{1}{4}R^3\right)k_m^2 S$ $+\frac{1}{r}\left(\frac{3R}{2b}-\frac{3R^2}{4b}\right)S$	$\frac{b}{r^2}\left(R-R^2+\frac{R^3}{4}\right)k_m^2 S$ $+\frac{1}{r}\left(2R-1-\frac{3R^2}{4}\right)S$	$\frac{1}{r^2}\left(\frac{3}{4}R^2-\frac{1}{4}R^3\right)k_m^2 S$ $+\frac{1}{r}\left(\frac{3R^2}{4b}-\frac{3R}{2b}\right)S$	$\frac{b}{r^2}\left(\frac{R^3}{4}-\frac{R^2}{2}\right)k_m^2 S$ $+\frac{1}{r}\left(R-\frac{3R^2}{4}\right)S$
$\frac{2}{r}\left(\frac{3R}{2b}-\frac{3R^2}{4b}\right)k_m C$ $+\frac{2}{r^2}\left(1-\frac{3}{4}R^2+\frac{1}{4}R^3\right)k_m C$	$\frac{2}{r}\left(-1+2R-\frac{3R^2}{4}\right)k_m C$ $+\frac{2b}{r^2}\left(R-R^2+\frac{R^3}{4}\right)k_m C$	$\frac{2}{r}\left(\frac{-3R}{2b}+\frac{3R^2}{4b}\right)k_m C$ $+\frac{2}{r^2}\left(\frac{3}{4}R^2-\frac{1}{4}R^3\right)k_m C$	$\frac{2}{r}\left(R-\frac{3R^2}{4}\right)k_m C$ $+\frac{2b}{r^2}\left(\frac{R^3}{4}-\frac{R^2}{2}\right)k_m C$

$$\left(k_m=\frac{m\pi}{\alpha},\qquad S=\sin k_m\theta,\qquad C=\cos k_m\theta\right).$$

Notation

w	displacement normal to plane of slab
$D_r, D_\theta, \nu_r, \nu_\theta, D_k$	cylindrical orthotropic constants and rigidities
r, θ	polar coordinates
w_i, ψ_i	displacements and rotations along side i of strip
w_{im}, ψ_{im}	displacement and rotation parameters of the mth term along side i of strip
P_i, M_i	shear forces and radial moments along side i of strip
P_{im}, M_{im}	shear force and radial moment parameters of the mth term along side i of strip

References

1. HUFFINGTON, N. J.: Theoretical Determination of Rigidity Properties of Orthogonally Stiffened Plates. T. of Appl. Mech., Vol. 23, 1956, p. 56.
2. YONEZAWA, H.: A Study of the Stiffness of Beam Bridges. Transactions, Jap. Soc. of Civil Engrs., Vol. 54, 1958, p. 43.
3. COULL, A. and DAS, P. C.: Analysis of Curved Bridge Decks. Proc. Instn. Civ. Engrs., Vol. 37, May 1967, p. 75–85.
4. CERADINI, G.: Théorie des pontes courbes à poutres multiples. IABSE, Vol. 25, 1965, p. 51–64.
5. YONEZAWA, H.: Moment and Force Vibrations in Curved Girder Bridges. Proc. ASCE, Vol. 88, No. EMI, Feb. 1962, p. 1–21.
6. CHEUNG, Y. K.: Analysis of Orthotropic Right Bridges by Finite Strip Method. 2nd Int. Sym. on Concrete Bridge Design, Chicago, March 1969.
7. LEKHNITSKII, S. G.: Anisotropic Plates. (Translated from 2nd Russian edition) Gordon and Breach Science Publishers, 1968.

Summary

An analysis of cylindrical orthotropic curved bridge slabs is presented in this paper. The slab is divided into a number of concentric circular strips, and the stiffness matrix of each strip, which is simply supported at its two ends, can be formulated by expressing the deflected form as a product of a Fourier series in the circumferential direction and a beam function in the radial direction. These individual stiffnesses are assembled and solved to give the nodal displacements and subsequently the internal moments. The method has a number of advantages. It is simple yet accurate, versatile yet easy to program and to execute. Furthermore, the program can be accomodated on a small computer such as the IBM 1130.

Résumé

Ce rapport présente un calcul des tabliers de ponts courbes à orthotropie circulaire. La dalle est divisée en un certain nombre de bandes circulaires concentriques simplement appuyées aux deux extrémités. La matrice de rigidité de chaque bande peut être formulée en exprimant la déformation comme un produit de séries de Fourier dans la direction tangentielle et comme une fonction de poutre dans la direction radiale. Ces rigidités individuelles sont assemblées et résolues, afin d'obtenir les déplacements nodaux et les moments internes. Cette méthode présente bon nombre d'avantages: Elle est simple, précise, facile à programmer et variée dans ses applications. De plus, le programme peut être adapté à de petits calculateurs électroniques tel que l'IBM 1130.

Zusammenfassung

Dieser Beitrag gibt eine Analyse der kreisförmig-orthotropen, gekrümmten Brückenplatten. Die Platte wird in eine Anzahl konzentrischer Streifen aufgeteilt. Die Steifigkeitsmatrix eines jeden Streifens, der an seinen zwei Enden einfach aufgelegt ist, ergibt sich, indem man die Biegefläche als ein Produkt einer Fourier-Reihe in Richtung des Umfanges mit einer Balkenfunktion in Richtung des Halbmessers anschreibt. Diese einzelnen Steifigkeiten werden zusammengefaßt; die Lösung gibt die Knotenverschiebungen und hernach die inneren Momente.

Dieses Verfahren zeigt eine Reihe von Vorteilen: Es ist einfach und trotzdem genau, vielseitig und trotzdem leicht zu programmieren und auszuführen. Weiterhin kann das Programm von sehr kleinen Elektronenrechnern, wie zum Beispiel der IBM 1130, bewältigt werden.